Cross-polarization Dynamics

Introduction

Low(er) gamma nuclei present a challenge to the NMR spectroscopist due to their small magnetogyric ratio, often low natural abundance, and typically long spin-lattice relaxation times. All three conspire to yield low sensitivity. The cross-polarization[1] experiment overcomes these challenges to offer high-sensitivity spectra of natural-abundance rare spins in the solid state by providing polarization transfer from abundant I spins.

The purpose here is to explain how the cross-polarization technique achieves this transfer. In particular, the origin of the dipolar Hamiltonian and its role in the polarization transfer is described. Signal enhancement is described in terms of a thermodynamic model, which has proven very useful. However, some limitations of the model are discussed. Finally, the dynamics of the process are illustrated with the experimental results from the ^{1}H-^{13}C cross polarization of adamantane and glycine. Consequences of experimental choices, such as Hartmann-Hahn[2] contact times and magic-angle spinning (MAS)[3,4], are shown. In particular, the issue of quantification is addressed.

The Dipolar Hamiltonian

The classical dipolar Hamiltonian derives from the calculation of the magnetic field of a nuclear spin and the interaction energy of a second nucleus with this field. The usual approach to this problem, often found in basic electricity and magnetism physics texts[5] and in some NMR texts[6], is to calculate the magnetic field due to a "distant circuit." Such an approach is reasonable, given the typical nuclear diameters relative to the bond lengths between neighboring nuclei. The typical diameter of a nucleus is on the order of 10^{-15} m, whereas typical bond lengths are of the order of 10^{-10} m. The five orders of magnitude difference in length scale between the nuclear separation and the "size" of the nuclei does fit the model of the first nucleus as a "distant circuit." This model shows that the magnetic field of a distant circuit does not depend upon its detailed geometry. It only depends upon its magnetic moment, $\vec{m}$. As a result, this calculation of a magnetic field due to a "distant circuit" describes the magnetic field due to a nuclear dipole very accurately.

The details of the calculation of the field are given below in Appendix I. The resulting magnetic field due to a "distant circuit" is

$$\vec{B}(\vec{r}) = \frac{\mu_0}{4\pi}\left[\frac{3(\vec{m}\cdot\vec{r}_2)\vec{r}_2}{r_2^5} - \frac{\vec{m}}{r_2^3}\right]. \qquad (1)$$

The energy of a second magnetic moment $\vec{m}'$ interacting with this magnetic field is given by $E = -\vec{m}' \cdot \vec{B}$, which gives the classical interaction energy

$$E = \frac{\mu_0}{4\pi}\left[\frac{\vec{m}' \cdot \vec{m}}{r_2^3} - \frac{3(\vec{m} \cdot \vec{r}_2)(\vec{m}' \cdot \vec{r}_2)}{r_2^5}\right] . \quad (2)$$

This is a convenient point for a brief discussion of units. There are two systems in common use to describe electromagnetic quantities, the Systeme Internationale (SI) of units and the gaussian (cgs) system.

In SI (mks) units, there is a distinction to the unit of the magnetic field and the magnetic induction. The quality that acts directly is the magnetic induction, $\vec{B}$, whereas the magnetic field, $\vec{H}$, is the directly measured quantity in practical electrical measurements. The magnetic field, $\vec{H}$, has units of amp/m. In SI, it is necessary to multiply the magnetic field, $\vec{H}$, by the permeability of free space, μ_0, (because the space between the nuclei is considered to be free space) to determine the magnetic induction $\vec{B}$ at the site of a dipole. The permeability has units of webers/ amp m. The magnetic induction, $\vec{B}$, is expressed in webers/m^2, also called teslas. The magnetic moment $\vec{m}$ has units of amp m^2.

In the gaussian (cgs) system, magnetic induction has units of gauss; and units are chosen such that in free space $\vec{B}$ and $\vec{H}$ are the same. However, the unit of magnetic field in the gaussian system is called the oersted.

In NMR spectroscopy it is usual to express energy differences by the equivalent frequency, given as ν in Hertz or as ω in radians/sec. The two units are related by the simple formula $\omega = 2\pi\nu$. These frequencies are related to equivlalent energies by Planck's relation, whether in SI or the gaussian system. In particular, the frequency is converted to the energy by multiplication by Planck's constant, *h*, or by Planck's constant divided by 2π, $h/2\pi$, for the circular frequency and radial frequency, respectively.

For conversion to the quantum mechanical problem, one replaces the classical magnetic moment with the quantum mechanical operator for it: $\vec{m} = \frac{\gamma h}{2\pi}\vec{I}$. With this change, the quantum mechanical dipolar Hamiltonian is written as

$$H_D = \sum_{j<k} \frac{h\gamma_j\gamma_k}{2\pi}\left[\frac{\vec{I}_j \cdot \vec{I}_k}{r_{jk}^3} - 3\frac{\left(\vec{I}_j \cdot \vec{r}_{jk}\right)\left(\vec{I}_k \cdot \vec{r}_{jk}\right)}{r_{jk}^5}\right]. \qquad (3)$$

Following Abragam[7], with θ and φ as the polar coordinates of the vector $\vec{r}$ and by using the raising and lowering operators $I_{\pm} = I_X \pm I_Y$, the dipolar Hamiltonian can be rewritten in terms of what is commonly called the "dipolar alphabet"

$$H_D = \sum_{j<k} \frac{h\gamma_j\gamma_k}{2\pi r_{jk}^3}\left[\vec{I}_j \cdot \vec{I}_k - 3\left\{I_{Zj}\cos\theta + \sin\theta\left(I_{Xj}\cos\varphi + I_{Yj}\sin\varphi\right)\right\}\times\left\{I_{Zk}\cos\theta + \sin\theta\left(I_{Xk}\cos\varphi + I_{Yk}\sin\varphi\right)\right\}\right]$$

$$H_D = \sum_{j<k} \frac{h\gamma_j\gamma_k}{2\pi r_{jk}^3}\left[\vec{I}_j \cdot \vec{I}_k - 3\left\{I_{Zj}\cos\theta + \frac{1}{2}\sin\theta\left(I_{+j}e^{-i\varphi} + I_{-j}e^{i\varphi}\right)\right\}\times\left\{I_{Zk}\cos\theta + \frac{1}{2}\sin\theta\left(I_{+k}e^{-i\varphi} + I_{-k}e^{i\varphi}\right)\right\}\right]$$

$$H_D = \sum_{j<k} \frac{h\gamma_j\gamma_k}{2\pi r_{jk}^3}[A+B+C+D+E+F] \qquad (4)$$

where

$$A = I_{Zj}I_{Zk}\left(1-3\cos^2\theta\right)$$

$$B = -\frac{1}{4}\left(1-3\cos^2\theta\right)\left(I_{+j}I_{-k} + I_{-j}I_{+k}\right) = \frac{1}{2}\left(1-3\cos^2\theta\right)\left(I_{Zj}I_{Zk} - \vec{I}_j \cdot \vec{I}_k\right)$$

$$C = -\frac{3}{2}\sin\theta\cos\theta\left(e^{-i\varphi}\right)\left(I_{Zj}I_{+k} + I_{Zk}I_{-j}\right)$$

$$D = C^* = -\frac{3}{2}\sin\theta\cos\theta\left(e^{+i\varphi}\right)\left(I_{Zj}I_{+k} + I_{Zk}I_{-j}\right)$$

$$E = -\frac{3}{4}\sin^2\theta\left(e^{-2i\varphi}\right)I_{+j}I_{+k}$$

$$F = E^* = -\frac{3}{4}\sin^2\theta\left(e^{2i\varphi}\right)I_{-j}I_{-k}$$

The reason for writing the dipolar Hamiltonian in this way is that it exposes how different parts of the Hamiltonian connect the various angular momentum levels. Of particular importance are the transitions in high magnetic field enabled by each term.

$$\begin{array}{llll} \text{A} & \Delta m_j = 0 & \Delta m_k = 0 & \Delta(m_j + m_k) = 0 \\ \text{B} & \Delta m_j = \pm 1 & \Delta m_j = -/+1 & \Delta(m_j + m_k) = 0 \\ \text{C} & \Delta m_j = \begin{cases} 0 \\ 1 \end{cases} & \Delta m_k = \begin{cases} 1 \\ 0 \end{cases} & \Delta(m_j + m_k) = 1 \\ \text{D} & \Delta m_j = \begin{cases} 0 \\ -1 \end{cases} & \Delta m_k = \begin{cases} -1 \\ 0 \end{cases} & \Delta(m_j + m_k) = -1 \\ \text{E} & \Delta m_j = 1 & \Delta m_k = 1 & \Delta(m_j + m_k) = 2 \\ \text{F} & \Delta m_j = -1 & \Delta m_k = -1 & \Delta(m_j + m_k) = -2 \end{array} \qquad (5)$$

For identical spins, *i.e.*, those subject to homonuclear dipolar coupling, the first two terms, A and B, describe the secular part of the interaction since they commute with the Zeeman Hamiltonian and thus will have simultaneous eigenstates with the Zeeman Hamiltonian. For inequivalent spins, *i.e.*, those subject to heteronuclear dipolar coupling, only the first term A commutes with the Zeeman Hamiltonian. In sufficiently high magnetic field these two terms are all that are required to determine the energy-level scheme for the system through first order and are often referred to as the "truncated" dipolar interactions[7].

The B term represents a process in which there exists a simultaneous flip of two spins in the opposite directions and is usually referred to as the "flip-flop" term. As mentioned, in the case of heteronuclear dipolar coupling, this term does not commute with the Zeeman Hamiltonian and is not included in the dipolar Hamiltonian. However, it is precisely this term that becomes important in the rotating frame and transfers polarization in the cross-polarization experiment. Kubo and Tomita[8] in their classic paper on the quantum mechanical treatment of NMR show that this term is better at energy transfer rather than at relaxation.

Another way to say this is to realize that the A and B terms yield energy differences corresponding to a frequency ω_0 for identical spins. The C, D, E, and F terms yield energy differences corresponding to frequencies of 0 and 2 ω_0. These last four terms are not important for consideration of transfer and are simply neglected in the development of cross-polarization transfer. That is, the A and B terms comprise the truncated dipolar Hamiltonian used in the theoretical development of cross polarization.

Cross-polarization Mechanism

The cross-polarization mechanism can be best explained and is mostly used in systems having abundant I spins with a higher magnetogyric ratio and rare S spins with a lower magnetogyric ratio. The most common experiment transfers energy from ^{1}H, as the I spins, to ^{13}C, as the S spins.

The pulse sequence for cross polarization from the abundant I spins to the rare S spins begins with a ninety-degree pulse on the I spins. The phases of the radiofrequency (rf) pulses are defined relative to the axes of the rotating frames of the nuclei. If the ninety-degree pulse applied to the I spins has a rf phase of X, then the I-spin magnetization ends up along the Y axis in the rotating frame at the end of the pulse, presuming that the magnetogyric ratio of the I spin is positive, or along the -Y axis, if the magnetogyric ratio is negative. The phase of the I-spin rf irradiation is then quickly switched to the Y phase to lock the magnetization along this axis while the S-spin rf irradiation is turned on simultaneously. During the simultaneous rf irradiation of both I and S spins, polarization is transferred from the abundant I spins to the rare S spins, creating S magnetization by draining polarization away from the I spins. Finally, at some later time, the S-spin rf irradiation is turned off and the transverse S-spin magnetization is measured while the I-spin rf irradiation remains on during the acquisition to provide decoupling.

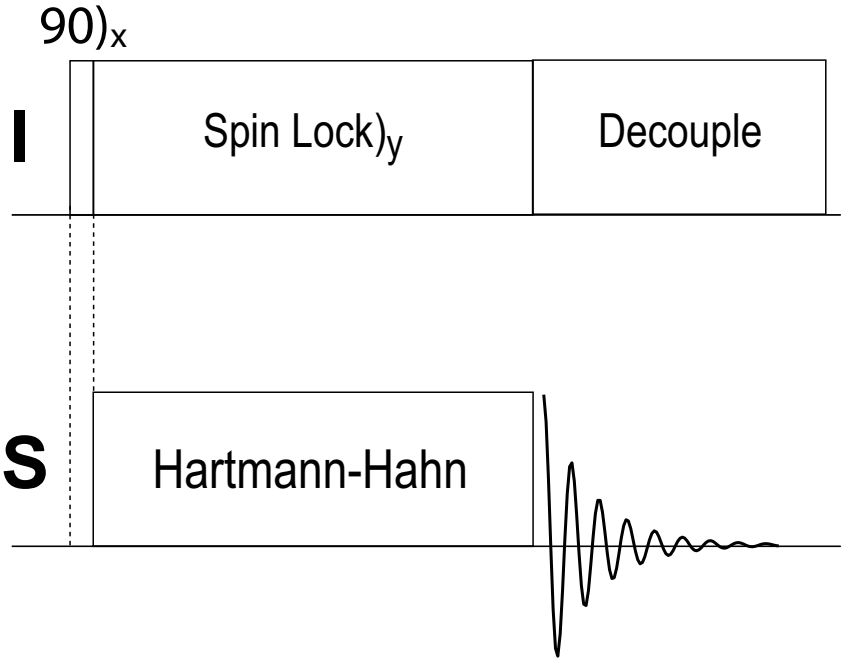

Quantum mechanics provides a description of the mechanism for cross polarization. One may think of the interactions in terms of Zeeman interactions. For the Zeeman interaction, the spin's energy levels are given by the dot product of the magnetic moment with the magnetic induction. It is not possible to have the same energy levels for nuclei with differing magnetogyric ratios in only one magnetic induction, such as the static magnetic field in the laboratory. The magnetogyric ratios of the I and S spins are constants. However, the energy levels for two differing nuclei can be made the same if

two magnetic inductions are used. In this case, the two magnetic inductions are the rotating components of the radiofrequency radiation applied to the I and S spins. By matching the Hartmann-Hahn condition $\omega_{I_{rf}} = \omega_{S_{rf}}$, the magnetic inductions from the rf pulses are of such a magnitude that the I and S spins have a common energy-level scheme in the rotating frame. That is, the energy levels for the I and S spins are matched in the rotating frames of the two different nuclei. The normally forbidden "flip-flop" transitions of the B term in the heteronuclear dipolar interaction are active in the rotating frame under these conditions, producing "allowed" simultaneous spin flips of the I and S spins with exchange of energy.

An alternative description of the mechanism of cross polarization can be given in terms of a thermodynamic model. Thermodynamics can be applied in the rotating frame since the Hamiltonian is effectively time-independent.

Thermodynamics applies to populations of energy states. Generally, as the temperature is lowered, states with lower energy become more populated compared to higher-energy states. This can be, in a simple way, thought of as an increase in order of the system. This is seen as a gas condenses into a liquid with an increase in local order as the temperature is lowered. Below the freezing point, the liquid becomes even more ordered as it forms a solid with the atoms or molecules now occupying specific lattice positions.

For NMR experiments the concept of spin temperature[9] must be explained to access the thermodynamic interpretation of cross polarization. The spin-lattice relaxation time T_1 has been defined as the time constant for the spin system to come into equilibrium with the lattice. The time constant T_2 roughly measures the time required for a spin system to come into some sort of internal quasi-equilibrium. Such quasi-equilibrium states may have energy-level populations very different from what they would be at the temperature of the lattice, but they ultimately return to the true equilibrium by spin-lattice transfer of energy. In the case of strong coupling between the spins, such as the dipolar interaction in solids, a spin temperature, *T*, different from the lattice temperature can be defined when $T_2 << T_1$. This temperature, defined through a Boltzmann factor, is nothing more than a description of relative populations of energy levels[10]. These temperatures, because they are related to Boltzmann factors, can then be used to give the probabilities of occupation of energy levels, allowing the calculation of physical properties as shown in Appendix II, when the system exhibits that spin temperature.

The cross-polarization experiment begins with the I magnetization, M_0, at equilibrium aligned with the static magnetic induction (which defines the Z axis) at the lattice temperature, T_L. For all practical purposes, there exists no net magnetization of the S spins (due to a small magnetogyric ratio and a long spin-lattice relaxation time), so it can be considered to be infinitely hot. Additionally, since the projection of the I magnetization in the X-Y plane is zero, the rotating-frame temperature of the I spins is also effectively infinite. (The absence of net magnetization in the X-Y plane is the random phase approximation in statistical mechanics. Alternatively, in quantum mechanics, the absence is due to the uncertainty principle of quantum mechanics, which does not allow the simultaneous measurement of all three components of the angular momentum.) After the ninety-degree pulse on the I spins and spin locking, the rotating-frame spin temperature, *T*, of the I spins is lowered to some value that depends on the thermal equilibrium magnetization, M_0, and the strength of the applied radiofrequency

induction that locks it (*vide infra*). The spin temperature of the I spins is reflective of the order in the I-spin manifold that is temporary.

In the high temperature approximation[11], in which the thermal energy given by the product of the Boltzmann constant with the temperature (kT) is greater than the separation of the magnetic energy levels, the magnetization, M_0 , displays a Curie law behavior. Following Slichter[12], this is shown in Appendix II. The magnetization is directly proportional to the magnetic induction B and inversely proportional to the temperature T,

$$\bar{M}_I = CB/T_I \qquad (6)$$

where C is the Curie Constant. Thus, specification of the temperature in a given magnetic induction is equivalent to specifying the magnetization and vice versa.

The initial I-spin magnetization, M_0, at thermal equilibrium with the lattice parallel to the large static laboratory magnetic induction is the same magnetization which is spin-locked after the ninety degree I-spin rf pulse. The much smaller magnetic induction of the spin-lock rf pulse requires a much lower spin temperature due to the Curie law.

$$M_0 = CB_0/T_I = CB_{rf}/T_f \qquad (7)$$

or

$$T_f = \frac{B_{rf}}{B_0} T_L \qquad (8)$$

where $\frac{B_{rf}}{B_0} << 1$.

So the final spin temperature is much colder than the initial temperature of the I spins at equilibrium in the static magnetic field. A simple calculation shows how effective this is at lowering the spin temperature. The lattice temperature is generally around 300 K. In a modern spectrometer, a typical magnetic induction, B_0, corresponds to a frequency of 500 MHz. The magnitude of a typical rf induction may correspond to a frequency of 80 kHz. Use of these values in the equation shows that, immediately after the ninety-degree pulse, the I spins are in a state of quasi-equilibrium corresponding to a temperature of about 0.05 K. This is an extremely cold system. Such a cold system should easily receive energy from a hotter system if placed in thermal contact with it.

Physically, the spin locking of the I-spin magnetization lowers the spin temperature of the I spins and provides I-spin magnetization (order) in the X-Y plane. At this point, the S spins are hot with no order in the X-Y plane. Thermal contact between the cold I spins and the hot S spins is made by applying a simultaneous rf pulse to the S spin system while the I spins are spin locked. Matching the Hartman-Hahn condition with these simultaneous rf pulses on both spin systems provides efficient thermal contact through

the flip-flop term of the dipolar interaction[13]. As the I spins warm, the S spins cool, generating S-spin magnetization in the X-Y plane aligned along the applied S rf induction. The I-spin rf pulse may be left on for decoupling as the S-spin signal is acquired.

Cross-polarization Enhancement

The transfer of energy from the hot S spins to the cold I spins, with consequent transfer of order from the I spins to the Spins, does not occur instantaneously. Following Mehring[14], assuming that the S spins are hot, *i.e.*, the S spins have a zero inverse temperature $1/T_S$ at t=0 (the beginning of the Hartmann-Hahn match) and neglecting spin-lattice relaxation, the I and S spins approach the same inverse temperature, $1/T_f$, exponentially

$$1/T_I(t) = \left(1/T_I - 1/T_f\right)e^{-t/T_{IS}} + 1/T_f \qquad (9)$$

and

$$1/T_S(t) = 1/T_f\,(1-e^{-t/T_{IS}}) \qquad (10)$$

where T_{IS} is the time constant for the exponential approach to the same final inverse temperature. Assuming energy conservation during this process, the final temperature can be estimated:

$$\frac{C_I B_{rfI}^2}{T_L} + \frac{C_S B_{rfS}^2}{T_S} = \frac{C_I B_{rfI}^2 + C_S B_{rfS}^2}{T_f} \qquad (11)$$

Assuming $1/T_S = 0$, then

$$\frac{T_L}{T_f} = \frac{1}{1+\varepsilon} \qquad (12)$$

where $\varepsilon = \frac{C_S B_{rfS}^2}{C_I B_{rfI}^2}$. With the Hartmann-Hahn condition $\gamma_I H_{rf_I} = \gamma_S H_{rf_S}$ and N_I, the number of abundant I spins, being much, much larger than N_S, the number of rare spins, then $\varepsilon = \frac{N_S S(S+1)}{N_I I(I+1)} << 1$. This expression for the final temperature in terms of the initial temperature can be plugged into the equation for the magnetization to give

$$M_I^f = \frac{1}{1+\varepsilon} M_I^i \qquad (13)$$

and

$$M_S^f = \frac{\gamma_I}{\gamma_S}\left(\frac{1}{1+\varepsilon}\right) M_{0S}. \qquad (14)$$

Since ε is small, the S spin magnetization can theoretically be enhanced by a factor of γ_I / γ_S. For example, for a system of carbons and protons, the theoretical prediction of the enhancement of the carbon magnetization under ideal conditions and with no relaxation is 3.98, almost a factor of 4.

Experimental Results

As a practical example, the effect of cross polarization from abundant protons to the 1.1% naturally abundant ^{13}C is shown below in the single-scan spectra below from a static sample of adamantane. The upfield methine resonance at 29.46 ppm is enhanced in the cross-polarization spectrum by a factor of 3.9 relative to the single ninety-degree pulse spectrum. In both spectra, ^{1}H decoupling was applied. The enhancement in the single scan is very close to the theoretical maximum calculated above.

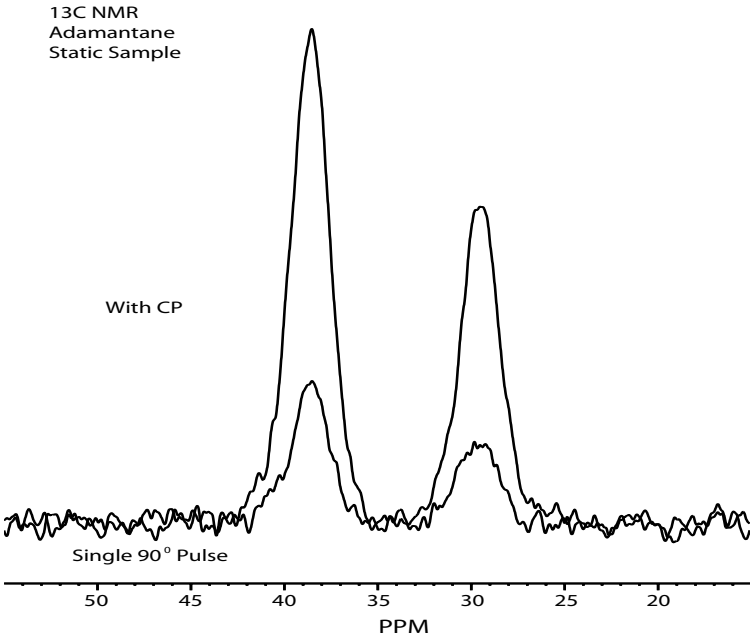

Additional enhancement of the ^{13}C signal relative to direct ^{13}C excitation is obtained when acquiring multiple scans in a given amount of time. The abundant spin system typically has a much shorter spin-lattice relaxation time as compared to the rare spin species. Since the cross-polarization experiment can be repeated on the basis of the spin-lattice relaxation rate of the abundant spin species, typically more scans can be acquired in a given time relative to the number of scans acquired with direct excitation of the rare spin species. Total enhancements on the order of 20 can be obtained in many cases. As a result, cross polarization is a widely used technique.

Cross polarization from the abundant I spins to the rare S spins requires matching the Hartmann-Hahn condition $\omega_{I_{rf}} = \omega_{S_{rf}}$, where $\omega_{rf} = \gamma_i B_{rfi}$ and γ_i is the magnetogyric ratio for the i^{th} nucleus. Simply adjusting the ninety-degree pulse widths of both the I and S spins to the same numerical value insures that one is at, or at least very close to, the necessary Hartmann-Hahn matching condition for the I-S cross polarization. This is easily seen by realizing that the flip angle θ is simply ωt_p, where t_p is the pulse width. If the flip angle is the same for both I and S spins when using the same pulse width, then $\omega_{I_{rf}} = \omega_{S_{rf}}$.

As an example of matching the Hartmann-Hahn condition for ^{1}H-^{13}C cross-polarization, the downfield methylene peak at 38.3 ppm of a static sample of adamantane has been repeatedly plotted with the same vertical scaling as a function of the ^{13}C rf power level used during the contact time for the match while the ^{1}H rf power level remains constant. The plot begins with highest power to the left-hand side, reduced in steps of 0.2 dB. The point of maximum signal is the point nearest the Hartmann-Hahn matching condition.

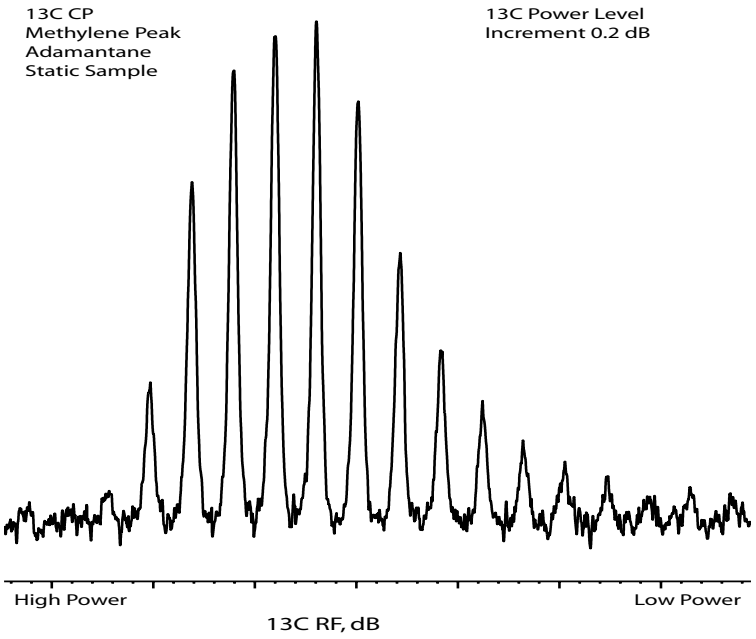

Thus far, the theoretical description given and the experimental results shown are for cross polarization with static samples. However, what is probably the most commonly

used cross-polarization experiment combines the technique with MAS to remove chemical-shift dispersion due to anisotropic interactions to provide a high-resolution solid-state spectrum. Since MAS can also average the heteronuclear dipolar coupling, MAS has some effect upon the cross-polarization experiment. Indeed this effect of the spinning on the cross-polarization process can be seen below in the plot for the methylene peak of adamantane as a function of the ^{13}C rf power when spinning the sample at a relatively modest speed of 3 kHz. The modulation of the peak amplitudes due to the influence of the MAS on the heteronuclear dipolar coupling is readily evident in this plot. The additional narrowing of the resonance line with the MAS is also noticeable. However most rigid solids require substantially faster spin rates than 3 kHz to observe the modulation.

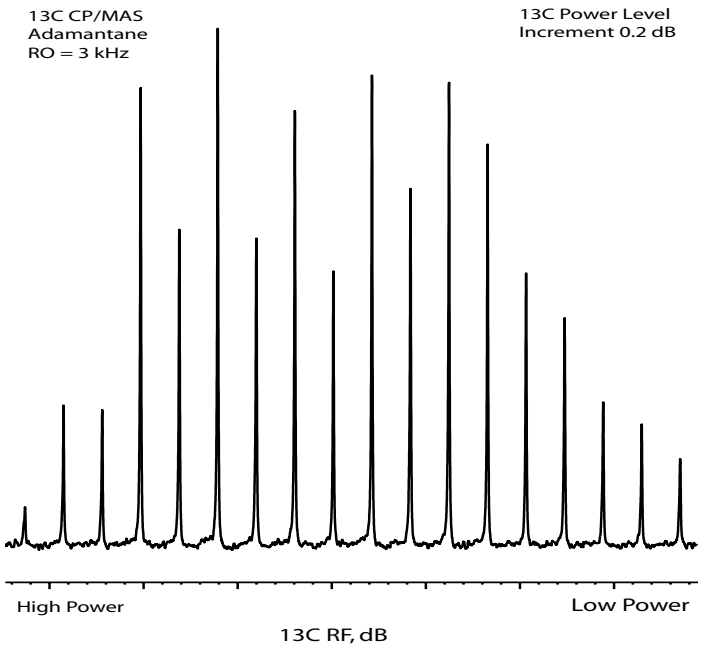

In the earlier discussion on inverse spin temperatures as given by Equations 9 and 10, no mechanism for relaxation of the I spins or the S spins was included. The general solution[14] for such a model is too complicated to be useful and has rarely been used in practice. Usually simplifying assumptions are made. Using $T_{1\rho I}$ as the time constant for I-spin relaxation under the spin-locking rf induction, $T_{1\rho S}$ as the time constant for S-spin relaxation under the spin-locking rf induction, and assuming that $\frac{N_S(\gamma_S B_{rfS})^2}{N_I(\gamma_I B_{rfI})^2} \approx 0$, the coupled differential equations can be solved[14] to give the intensity of S-spin magnetization *M(t)* as

$$M(t) = \frac{M_0}{\left(1 + \frac{T_{IS}}{T_{1\rho S}} - \frac{T_{IS}}{T_{1\rho I}}\right)}\left(e^{-(t/T_{1\rho I})} - e^{(t/T_{IS} + t/T_{1\rho S})}\right) \quad . \qquad (15)$$

Use of equation 15 in variable contact time measurements often requires additional experiments to separately measure the additional quantities such as the S-spin rotating frame relaxation time, $T_{1\rho S}$. However, with the further assumption that $T_{IS}/T_{1\rho S} \approx 0$, this reduces to one of the more commonly used solutions with which to fit variable contact time experiments

$$M(t) = \frac{M_0}{\left(1 - \frac{T_{IS}}{T_{1\rho I}}\right)}\left(e^{-(t/T_{1\rho I})} - e^{(t/T_{IS})}\right) \quad . \qquad (16)$$

The behavior of the intensity of both the methylene and methine resonances in a static sample of adamantane as a function of contact time is identical. This is consistent with the random isotropic motion of the adamantane molecule in the plastic crystal at ambient temperature averaging out the intramolecular dipolar interaction and the intermolecular dipolar interaction providing the cross polarization. Otherwise, the two protons on the methylene should provide a faster increase in intensity relative to the singly protonated methine.

As a distinctly different example, the ^{13}C magnetization, *M(t)*, for the carbonyl of glycine is plotted as a function of the Hartmann-Hahn contact time in a ^{13}C CP/MAS experiment. The rf field strength is 62.5 kHz. The fitted equation 16 yields a T_{IS} of 0.52 ms and a ^1H $T_{1\rho}$ of 54 ms.

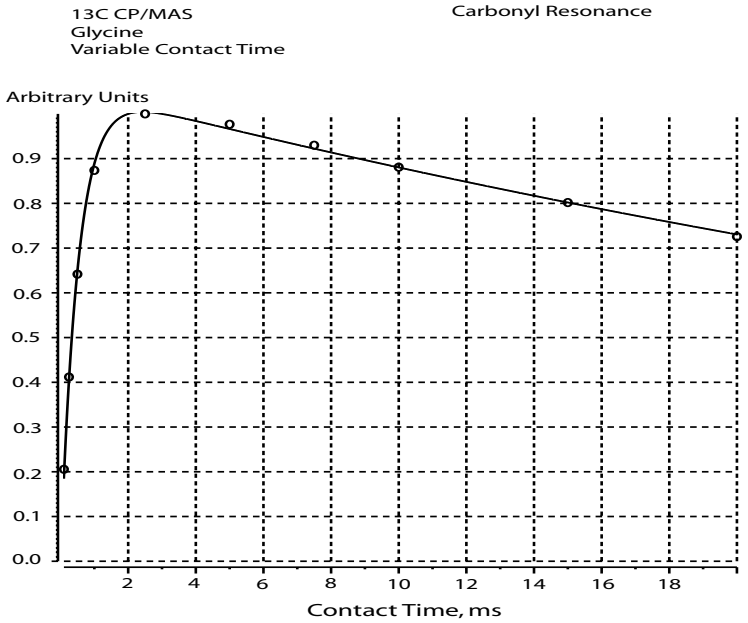

It should be noted that the time constant T_{IS} for this polarization transfer to the non-protonated carbonyl is much longer than the approximate[15] T_{IS} of 0.08 ms for the protonated methylene of glycine. The slow increase in intensity of the carbonyl relative

to that of the methylene carbon of glycine can easily be seen in the three ^{13}C CP/MAS spectra with contact times of 0.5, 1, and 5 ms shown below.

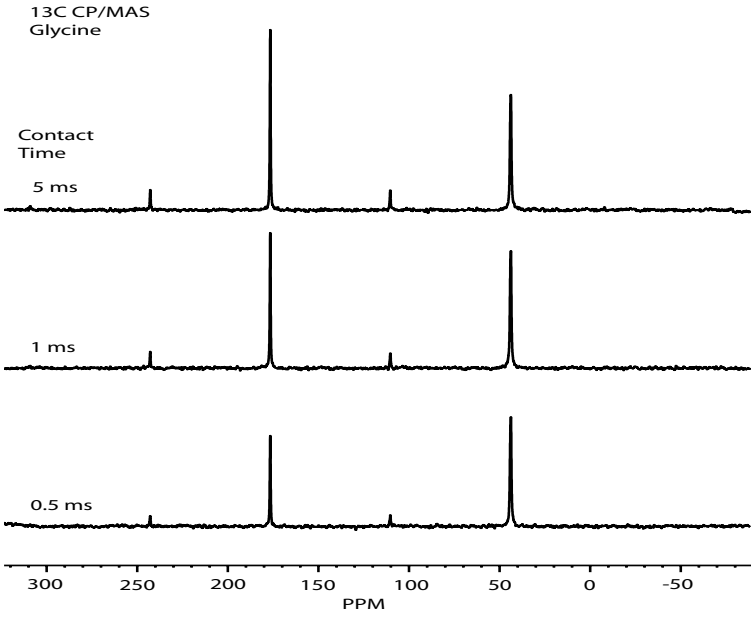

The increase in intensity is strongly dependent upon the local environment of the nucleus in the molecule. As shown, the non-protonated carbonyl reaches its maximum intensity more slowly than the protonated methylene carbon. However, the decays of the variable contact curves for each carbon resonance are governed by the single proton $T_{1\rho H}$. The protons show strong homonculear dipolar coupling in the molecule and, hence, show only one relaxation time constant. The buildup of S-spin magnetization on short time scales is very sensitive to the immediate environment of the nucleus in the molecule and might be described as a "microscopic" view of the immediate local surroundings of the nucleus. The decay of the S-spin magnetization on longer time scales due to the ^1H $T_{1\rho}$ reflects more on the molecule as a whole due to strong homonuclear dipolar interactions and provides more of a "macroscopic" view of the molecule.

This is important for the acquisition of quantitative, or perhaps what is more precisely called semi-quantitative, data. The maximum signal for each peak is reached roughly around $3T_{IS}$, which is likely to differ substantially for various sites within a molecule. It is necessary to ensure an adequately long contact time, greater than three times the longest T_{IS}, for quantification. This quantification is gained at the expense of some deterioration in the signal-to-noise ratio. When MAS is also used, it is necessary to include the areas of any spinning sidebands with the resonance of interest to get the total area. This is shown below in a ^{13}C CP/MAS spectrum of glycine acquired with a sample rotation rate of 5 kHz. It should be noted that sideband-suppression techniques such as TOSS[16] do not refocus the sideband intensity into the center band. In the limit of high spinning speeds and low sideband intensity, TOSS loses a contribution to the isotropic peak of about half of the combined area of the sidebands. As a result, techniques such as

TOSS are not quantitative, becoming even less quantitative for situations in which the chemical shift anisotropies are significantly different.

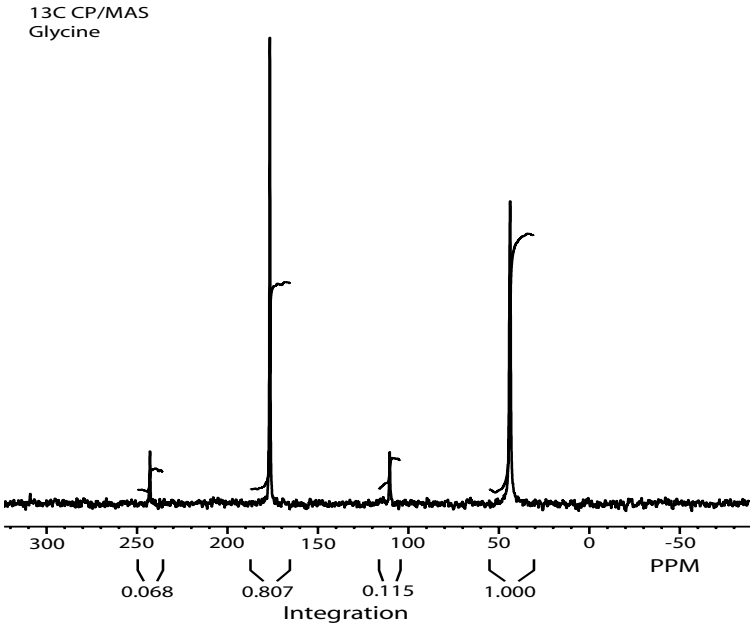

The important spin-relaxation parameters in the cross-polarization experiment are the spin-lattice relaxation times in the rotating frames ($T_{1\rho}$) of both the I and S spins. If the I-spin $T_{1\rho}$ is too short, then the I spins cannot be spin-locked in the rf field and thus cooled down. Of course, the I-spin $T_{1\rho}$ will also be too short if the I-spin spin-lattice relaxation time T_1 is too short, as $T_{1\rho}$ cannot be greater than T_1. The I-spins will have equilibrated back to the original spin temperature before polarization transfer to the S spins can occur. In other words, the polarization transfer takes time to occur. Cross polarization occurs only if the entire spin system has reasonably long relaxation times.

The role of relaxation times in quantification becomes very important, especially for quantification of mixtures or polymers which may have both crystalline and amorphous domains exhibiting different relaxation parameters. In these cases, relaxation parameters can vary from resonance to resonance. It is then necessary to analyze the complete magnetization-evolution curve as a function of the contact time when using cross polarization as a quantitative tool[17]. In this case, the total magnetization, M_0, for each resonance can be extracted by fitting the equation for the magnetization as a function of the contact time to the experimental data. However, as pointed out[17], it is necessary to have an appropriate model which accurately describes the contact time behavior for each resonance.

The difficulty with short relaxation times occurs for alpha glycine[18] when using rf fields of 62.5 kHz. As the temperature of the sample is lowered from ambient temperature to 213 K, the ^{13}C CP/MAS signal simply disappears, as shown below. In this case, the ^1H T_1 of 0.25 s at ambient temperature increases to 23 s at 213 K while the ^1H $T_{1\rho}$ of 54 ms at ambient temperature shortens to 0.6 ms at 213 K. With a Hartmann-Hahn contact time of 3 ms, the ^{13}C CP/MAS signal from glycine is lost. This shortened ^1H $T_{1\rho}$ results from the hindered rotation of the $-NH_3$ group. At this temperature, it provides an

effective relaxation mechanism in the kHz regime. In short, as shown here for glycine and earlier for adamantane, molecular motion plays an important role in cross-polarization.

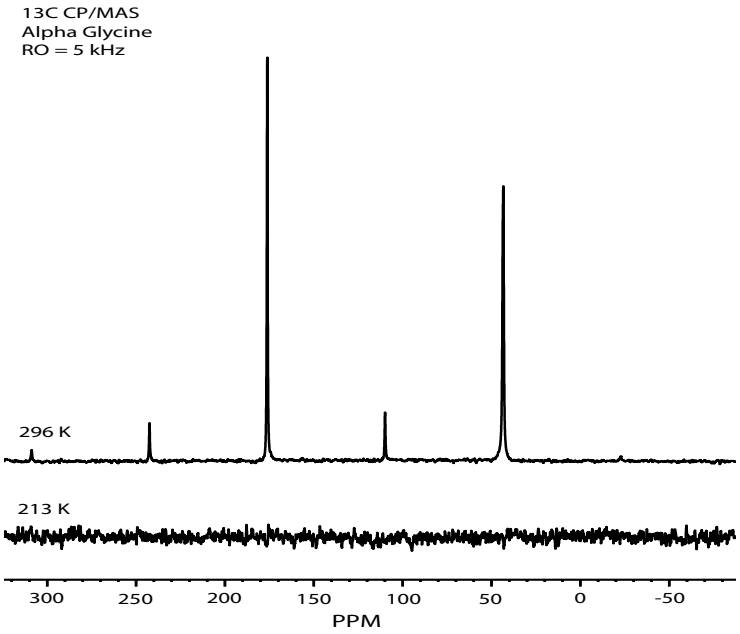

Cross-polarization signals can still often be obtained in such situations like that of glycine. However, this usually requires a change in the data-acquisition conditions. For glycine, a much shorter contact time, on the order of tens or hundreds of μs, can be used for the polarization transfer contact time. In addition, the use of a higher rf field strength, such that the $T_{1\rho}$ is changed, may also help.

An Overview

The thermodynamic analysis given for the cross-polarization experiment[1b] followed the analysis of earlier double-resonance experiments[19] in solids in which the S resonance, difficult to observe directly, is detected indirectly through its effect on the I spins. Such analyses are ultimately based on Redfield's concept[20] of a spin temperature in the rotating frame of reference. Slichter[12] refers to Redfield's paper as "one of the most important papers ever written on magnetic resonance."

The combination of MAS with cross polarization was addressed early[21]. At that time, the effect of MAS on cross polarization for most rigid solid materials seemed negligible. While MAS was effective at narrowing the inhomogeneously broadened chemical shift dispersions brought on by substantial chemical-shielding anisotropies, most spin rates were significantly smaller than the homogeneously broadened homonuclear dipolar linewidths of the protons. The modulation of the heteronuclear dipolar coupling by homonuclear dipolar fluctuations is simply much larger than the coherent modulation by the relatively slow sample spinning. As technology provided ever faster MAS spin rates,

the theory of CP/MAS was revisited[22,23] to accommodate "fast spinning." For rapid MAS, the most efficient transfer is usually observed under the modified Hartman-Hahn condition $\omega_{rfS} - \omega_{rfI} = n\upsilon_r$. That is, transfer is most efficient at a multiple of the sample spin rate ν_r, usually $n = \pm 1, \pm 2$. However, this presents an experimental challenge. The Hartmann-Hahn matching condition becomes very narrow and is susceptible to both rf inhomogeneities and instability in the spinning speed. Techniques such as variable-amplitude cross polarization[24] were developed to address concerns.

Limitations of this classic thermodynamic description of cross polarization were evident early on when strong transient oscillations were observed in the ^{13}C magnetization as a function of the contact time in a ferrocene single crystal[25]. In this case, there is a dominant dipolar interaction, which causes a deviation from the typical Gaussian line shapes in solids and leads to an oscillatory polarization transfer. Indeed, deviations from the exponential-rise-exponential decay model of polarization transfer as given by equation 16 were reported[26] for the α-carbon of polycrystalline glycine. This deviation for the methylene resonance in polycrystalline glycine in a variable contact time experiment is shown below. This contrasts with the good fit of equation 16 to the carbonyl resonance for glycine shown in the previous section. In these cases where equation 16 fails to adequately fit the observed data, variations of the I-I*-S model[27] are used to describe a dominant dipolar coupling to the S spin which leads to oscillatory behavior in the polarization transfer that is gradually damped as spin diffusion occurs among the abundant I spins.

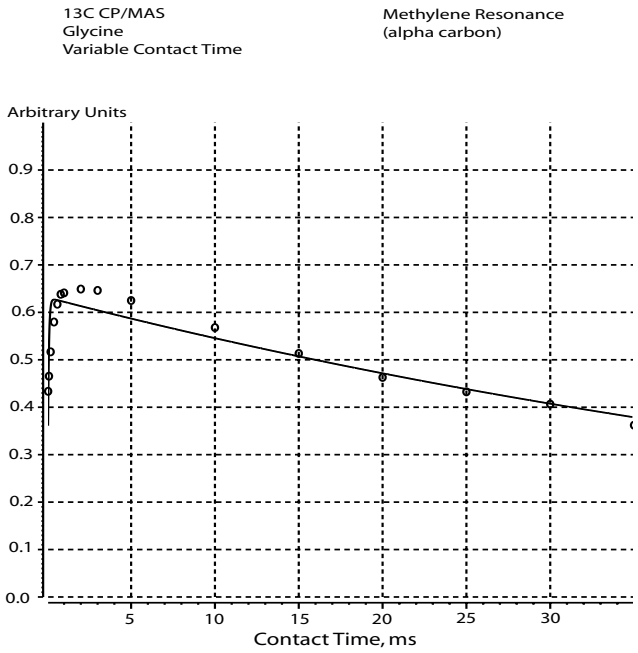

Citing concerns of "weakness" in the spin-temperature approach, a theory based on the quantum Liouville equation[28] has been proposed for CP/MAS. The specific concerns with the thermodynamic approach involved "no basis for an equilibrium to be obtained and thus no basis for assuming a thermal distribution" (as the spin system shows little or no relaxation during the experiment) and the fact that the Hamiltonian is still time-

dependent if MAS is performed (which questions the thermal equilibrium in the doubly-rotating frame).

Numerous examples of variable contact time experiments and analyses to study magnetization transfer of particular functionalities in various materials are in a recent review article[27]. In particular, many materials science applications are given. Such kinetic studies (which depend strongly upon dipolar interactions and, hence, on the I-S distance for nuclei like ^{1}H and ^{13}C) provide information on spatial orientation, mobility, separation of domains, and differentiation between protonated and non-protonated carbons. Other recent studies included amino acids[29] and coal[30].

The cross-polarization experiment using the heteronuclear dipolar interaction is widely used in solid-state NMR, especially for spin-½ nuclei with polarization transfer from abundant ^{1}H to enhance the sensitivity of such rare spin species as ^{13}C, ^{29}Si, and ^{15}N. In the solid state, it is also possible to cross polarize to or from half-integer quadrupolar nuclei[28]. However, such experiments are typically difficult due to the challenges presented by the spin dynamics involved in spin locking and polarization transfer via the quadrupolar interaction. This difficulty is exacerbated with the addition of MAS. These difficulties arise in polycrystalline materials from the polarization transfer being strongly anisotropic with respect to crystallite orientation in the magnetic field. The polarization transfer also depends upon the relative size of the quadrupolar coupling constants, the amplitudes of the rf inductions, the spinning speed, and the resonance offsets. The poor polarization transfer efficiency, as compared with that achievable for spin-½ nuclei, means that cross polarization for quadrupolar nuclei is primarily a means of spectral editing as opposed to a means of signal enhancement.

References

1. a) A. Pines, M. G. Gibby, and J. S. Waugh, J. Chem. Phys. 1972, 56(4): 1776-1777. "Proton-Enhanced Nuclear Induction Spectroscopy. A Method for High Resolution NMR of Dilute Spins in Solids."

b) A. Pines, M. G. Gibby, and J. S. Waugh, J. Chem. Phys. 1973, 59(2): 569-590. "Proton-enhanced NMR of dilute spins in solids."

2. S. R. Hartmann and E. L. Hahn, Phys. Rev. 1962, 128(5): 2042-2053. "Nuclear Double Resonance in the Rotating Frame."

3. a) E. R. Andrew, A. Bradbury, and R. G. Eades, Nature 1958, 182: 1659. "Nuclear Magnetic Resonance Spectra from a Crystal rotated at High Speed."

b) E. R. Andrew, A. Bradbury, and R. G. Eades, Nature 1959, 183: 1802-1803. "Removal of Dipolar Broadening of Nuclear Magnetic Resonance Spectra of Solids by Specimen Rotation."

4. I. J. Lowe, Phys. Rev. Letters 1959, 2(7):285-287. "Free Induction Decays of Rotating Solids."

5. e.g., J. R. Reitz and F. J. Milford, *Foundations of Electromagnetic Theory*, Second Edition, Addison-Wesley Publishing Company, Reading, Massachusetts, 1967, pp. 163-165.

6. e.g., B. C. Gerstein and C. R. Dybowski, *Transient Techniques in NMR of Solids -- An Introduction to Theory and Practice*, Academic Press, Inc., Orlando, Florida, 1985, pp.277-281.

7. J. H. Van Vleck, Phys. Rev., 1948, 74(9), 1168-1183. "The Dipolar Broadening of Magnetic Resonance Lines in Crystals."

8. R. Kubo and K. Tomita, J. Physical Society Japan, 1954, 9(6), 888-919. "A General Theory of Magnetic Resonance Absorption."

9. A. Abragam, *The Principles of Nuclear Magnetism*, Oxford University Press, Oxford, 1961, pp. 103-105, 133-158.

10. Having populations different from the equilibrium populations, at least temporarily, is seen in many experiments. One example which exhibits this effect is the laser, in which population levels are inverted, a fact that corresponds to a negative temperature, if one assumes that Boltzmann statistics apply to such systems.

11. a) J. H. Van Vleck, J. Chem. Phys. 1937, 5: 320337. "The Influence of Dipole-Dipole Coupling on the Specific Heat and Susceptibility of a Paramagnetic Salt."
b) J. H. Van Vleck, Phys. Rev. 1940, 57: 426-447. "Paramagnetic Relaxation Times for Titanium and Chrome Alum."

12. C. P. Slichter, *Principles of Magnetic Resonance*, Second Edition, Springer-Verlag, Berlin, 1978, pp.137-139, 188-200.

13. At any time, there is thermal contact with other degrees of freedom. However, the efficiency of the thermal contact under Hartmann-Hahn conditions allows the transfer before equilibrium with the other degrees of freedom transpires.

14. M. Mehring, "High Resolution NMR Spectroscopy in Solids," in *NMR 11: Basic Principles and Progress*, edited by P. Diehl, E. Fluck, and R. Kosfeld, Springer-Verlag, Berlin, 1976, pp. 113-119.

15. The growth in intensity for the protonated methylene resonance of glycine deviates from the exponential model in equation 16. This is discussed further in the limitations of the classic thermodynamic model in the Overview section.

16. W. T. Dixon, J. Schaeffer, M. D. Sefcik, E. O. Stejskal, and R. A. McKay, J. Magn. Reson. 1982, 49: 341-345. "Total Suppression of Sidebands in CPMAS C-13 NMR."

17. D. G. Rethwisch, M. A. Jacintha, and C. R. Dybowski, Anal. Chim. Acta 1993, 283: 1033-1043. "Quantification of ^{13}C in solids using CPMAS-DD-NMR spectroscopy."

18. R. E. Taylor, Concepts Magn. Reson. 2004, 22A(2): 79-89. "^{13}C CP/MAS: Application to Glycine."

19. F. M. Lurie and C. P. Slichter, Phys. Rev. 1964, 133(4A): A1108-A1122. "Spin Temperature in Nuclear Double Resonance."

20. A. G. Redfield, Phys. Rev. 1955, 98(6): 1787-1809. "Nuclear Magnetic Resonance Saturation and Rotary Saturation in Solids."

21. E. O Stejskal, J. Shaeffer, and J. Waugh, J. Magn. Reson. 1977, 28: 105-112. "Magic-Angle Spinning and Polarization Transfer in Proton-Enhanced NMR."

22. B. H. Meier, Chem. Phys. Letters 1992, 188(3,4): 201-207. "Cross polarization under fast magic angle spinning: thermodynamical considerations."

23. a) S. Ding, C. A. McDoweel, and C. Ye, J. Magn. Reson. Series A, 1994, 109: 1-5. "Cross Polarization at the Slow-Correlation Limit."
b) S. Ding, C. A. McDoweel, and C. Ye, J. Magn. Reson. Series A, 1994, 109: 6-13. "Dynamic Theory of Cross Polarization in solids under High-Speed Magic-Angle Spinning."

24. O. B. Peersen, X. Wu, I. Kustanovich, and S. O. Smith, J. Magn. Reson.Series A 1993, 104: 334-339. "Variable-Amplitude Cross-Polarization MAS NMR."

25. L. Müller, A. Kumar, T. Baumann, and R. R. Ernst, Phys. Rev. Letters 1974, 32(25): 1402-1406. "Transient Oscillations in NMR Cross-Polarization Experiments in Solids."

26. J. M Smith, C. Dybowski, and S. Bai, Solid State NMR, 2005, 27: 149-154. "Kinetics of NMR spin-lock polarization transfer in crystalline and spin-lattice relaxation of amino acids."

27. W. Kolodziejski and J. Klinowski, Chem. Rev. 2002, 102: 613-628. "Kinetics of Cross-Polarization in Solid-State NMR: A Guide for Chemists."

28. F. Marica and R. F. Snider, Solid State NMR 2003, 23: 28-49. "An analytical formulation of CPMAS."

29. K. Abelmann, L. U. Totsche, H. Knicker, and I. Kögel-Knabner, Solid State NMR, 2004, 25: 252-266. "CP dynamics of heterogeneous organic material: characterization of molecular domains in coals."

30. J.-P. Amoureux and M. Pruski, Molecuclar Phys. 2002, 100(10): 1595-1613. "Theoretical and experimental assessment of single- and multiple-quantum cross-polarization in solid state NMR."

Appendix I

The magnetic field at any point in space can be represented in terms of the magnetic vector potential $\vec{A}$, which is determined by the current density $\vec{J}(\vec{r})$. The magnetic induction is the curl of the vector potential, $\vec{B} = \vec{\nabla} \times \vec{A}$. This results from one of Maxwell's four equations requiring the divergence of $\vec{B}$ to be zero and from vector analysis where the divergence of the curl of any vector is zero.

Another of Maxwell's equations relates the magnetic field to the current density by $\vec{\nabla} \times \vec{B} = \vec{\nabla} \times \vec{\nabla} \times \vec{A} = \mu_0 \vec{J}$. Using the vector identity $\vec{\nabla} \times (\vec{\nabla} \times \vec{A}) = \vec{\nabla}(\vec{\nabla} \cdot \vec{A}) - \nabla^2 \vec{A}$ and physically arguing that the divergence of $\vec{A}$, that is $\vec{\nabla} \cdot \vec{A}$, can be set to zero without affecting the curl yields Poisson's Equation, $-\nabla^2 \vec{A} = -\mu_0 \vec{J}$. With the substitution $\vec{J}\, dv = Id\vec{r}$, the solution to Poisson's Equation is $\vec{A}(\vec{r}) = \frac{\mu_0 I}{4\pi} \oint \frac{d\vec{r}}{\left| \vec{r}_2 - \vec{r}_1 \right|}$.

Expanding $\left| \vec{r}_2 - \vec{r}_1 \right|^{-1}$ and using the identity $\vec{r}_1 \times d\vec{r}_1 \times \vec{r}_2 = -\vec{r}_1 (\vec{r}_2 \cdot d\vec{r}_1) + d\vec{r}_1 (\vec{r}_1 \cdot \vec{r}2)$ allow the vector potential to be written as $\vec{A}(\vec{r}) = \frac{\mu_0}{4\pi} \left[\frac{I}{2} \oint \vec{r}_1 \times d\vec{r}_1 \right] \times \frac{\vec{r}_2}{r_2^3}$, or in terms of the magnetic moment $\vec{m}$, $\vec{A}(\vec{r}) = \frac{\mu_0}{4\pi} \frac{\vec{m} \times \vec{r}_2}{r_2^3}$. Using the vector identity $\vec{\nabla} \times (\vec{F} \times \vec{G}) = \vec{F} \vec{\nabla} \cdot \vec{G} - \vec{G} \vec{\nabla} \cdot \vec{F} + (\vec{G} \cdot \vec{\nabla}) \vec{F} - (\vec{F} \cdot \vec{\nabla}) \vec{G}$, the magnetic field can be calculated from the curl of the vector potential yielding $\vec{B}(\vec{r}) = \frac{\mu_0}{4\pi} \left[\frac{3(\vec{m} \cdot \vec{r}_2)\vec{r}_2}{r_2^5} - \frac{\vec{m}}{r_2^3} \right]$. The important point is that the magnetic field of a distant circuit does not depend upon its detailed geometry but can be expressed in terms of its magnetic moment.

The Zeeman energy of a second magnetic moment $\vec{m}'$ interacting with this magnetic field is $E = -\vec{m}' \cdot \vec{B}(\vec{r})$, as given earlier in equation 2,

$$E = \frac{\mu_0}{4\pi}\left[\frac{\vec{m}'\cdot\vec{m}}{r_2^3} - \frac{3(\vec{m}\cdot\vec{r}_2)(\vec{m}'\cdot\vec{r}_2)}{r_2^5}\right] \qquad (2).$$

To understand the origin of the nomenclature of this "magnetic dipolar interaction," it is enlightening to explicitly compare this result with that derived for an electric dipole. In the case of an electric dipole, the necessary mathematics are more straightforward.

The form for the electrical dipolar interaction is derived by determining the field due to the electric dipole at some point P, as shown below. The field is the gradient of the scalar potential $\vec{E} = \vec{\nabla} V$, where $V = q(\frac{1}{r_1} - \frac{1}{r_2})$ for a << r.

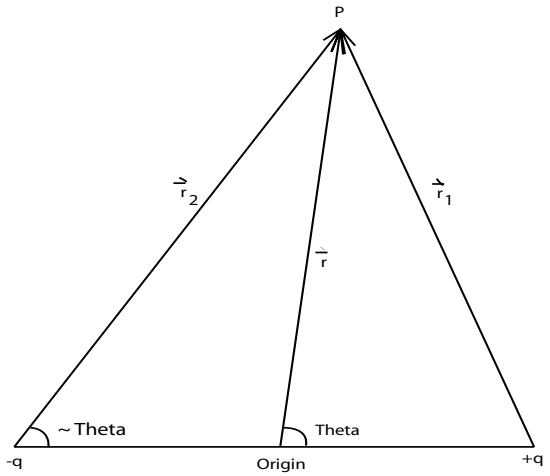

Electrical Dipole
at Point P

Expressing the potential in terms of r yields $V = q\left\{\frac{1}{r - \frac{a}{2}\cos\vartheta} - \frac{1}{r + \frac{a}{2}\cos\vartheta}\right\}$.

However, $V = q\left\{\dfrac{a\cdot\cos\vartheta}{r^2 - \dfrac{a^2}{4}\cos^2\vartheta}\right\} \approx \dfrac{\left|\vec{m}\right|\cos\vartheta}{r^2} = \dfrac{\vec{m}\cdot\vec{r}}{r^3}$, where a << r and the dipole moment is defined by $\vec{m} = q\vec{a}$. Since $-\vec{\nabla}\left(\dfrac{1}{r}\right) = \dfrac{\vec{r}}{r^3}$, the potential can be written as $V = -\vec{m}\cdot\vec{\nabla}\left(\dfrac{1}{r}\right)$. Using the vector identity $\vec{\nabla}\left(\vec{F}\cdot\vec{G}\right) = \left(\vec{F}\cdot\vec{\nabla}\right)\vec{G} + \left(\vec{G}\cdot\vec{\nabla}\right)\vec{F} + \vec{F}\times\vec{\nabla}\times\vec{G} + \vec{G}\times\vec{\nabla}\times\vec{F}$ and realizing that $\vec{m} = q\vec{a}$ = a constant, then the field due to a dipole is $\vec{E} = \left(\vec{m}\cdot\vec{\nabla}\right)\vec{\nabla}\left(\dfrac{1}{r}\right)$.

The energy of a second dipole $\vec{m}'$ interacting with this field is given by $E = -\vec{m}'\cdot\vec{E}$. $E = \sum_i\sum_j m_i' m_j \dfrac{\partial}{\partial q_j}\dfrac{q_i}{r^3}$, where q = x, y, z. Using $\dfrac{\partial}{\partial q_j}\dfrac{q_i}{r^3} = \dfrac{\delta_{ij}}{r^3} - \dfrac{3q_iq_j}{r^5}$ gives

$$E = \frac{\vec{m}'\cdot\vec{m}}{r^3} - \frac{3\left(\vec{m}'\cdot\vec{r}\right)\left(\vec{m}\cdot\vec{r}\right)}{r^5}.$$

Since the magnetic interaction given in equation (2) has the same functional form as that of the electrical dipole interaction, equation (2) is usually referred to as the magnetic dipole interaction.

Appendix II

Consider a spin system in thermal equilibrium with a reservoir of temperature T. The various states n of the total system are occupied with fractional probabilities p_n given by the Boltzmann factor

$$p_n = \frac{1}{Z}e^{-E_n/kT}$$

where Z is the partition function, k is Boltzmann's constant, and E_n is the energy of the state. The partition function Z can be calculated[11a] without solving for the energies and eigenvalues of the Hamiltonian by expanding the partition function in powers of 1/T. In other words,

$$Z = \sum_n e^{-E_n/kT} = \sum_n \left\langle n \left| e^{-H/kT} \right| n \right\rangle = Tr\left\{ e^{-H/kT} \right\}$$

Expanding the exponential in a power series,

$$Z = Tr\left\{ \left(1 - H/kT + \frac{1}{2}(H/kT)^2 + ... \right) \right\} = (2I+1)^N + \frac{1}{2(kT)^2} Tr\{H^2\} + ...$$

in which the Tr{H} = 0 for both the Zeeman and dipolar interactions. The average energy $\bar{E}$ and the magnetization $\bar{M}_z$ are given by

$$\bar{E} = \sum_n p_n E_n$$

and

$$\bar{M}_z = \sum_n \frac{\gamma\hbar}{2\pi} (n|I_z|n) p_n \ .$$

In the high temperature limit[11b] with the magnetic energy levels being much smaller than kT, then terms of $1/(kT)^2$ and higher can be ignored to yield

$$p_n = Z^{-1}\left(1 - E_n/kT \right)$$

which results in the average energy and magnetization of

$$\bar{E} = -CB^2/T$$

and

$$\bar{M} = CB/T$$

where $C = \frac{1}{3k}\left(\frac{N\gamma^2 h^2 I(I+1)}{(2\pi)^2} \right)$, the Curie constant, and $H = -\gamma \vec{B} \cdot \vec{I}$ with $\vec{B}$ being the magnetic induction. This high temperature approximation is typically valid for spin-½ nuclei above 4 K.